Phys. Status Solidi C **6**, No. S2, S413–S416 (2009) / **DOI** 10.1002/pssc.200880967

physica status solidi c
www.pss-c.com
current topics in solid state physics

Electrical properties of InGaN-Si heterojunctions

Joel W. Ager III[*,1], Lothar A. Reichertz[1], Yi Cui[1], Yaroslav E. Romanyuk[1,2], Daniel Kreier[1,2], Stephen R. Leone[1,2], Kin Man Yu[1], William J. Schaff[3], and Wladyslaw Walukiewicz[1]

[1] Lawrence Berkeley National Laboratory, 1 Cyclotron Rd., Berkeley, CA 94720, USA
[2] Departments of Chemistry and Physics, University of California at Berkeley, Berkeley, CA 94720, USA
[3] Department of Electrical Engineering and Computer Science, Cornell University, Ithaca, NY 14853, USA

Received 30 September 2008, revised 20 October 2008, accepted 26 October 2008
Published online 29 January 2009

PACS 71.55.Eq, 72.10.Fk, 73.40.Ty, 81.15.Hi, 84.60.Bk

[*] Corresponding author: e-mail JWAger@lbl.gov

The electrical transport properties of n-$In_xGa_{1-x}N$ heterojunctions with Si(111) were investigated. InGaN films were grown by molecular beam epitaxy and either an AlN or Si_3N_4 buffer layer was used. For x in the range of 15-45%, an ohmic junction is obtained with p-type Si and a rectifying junction is formed with n-type Si. The n-InGaN/n-Si heterojunction device functions as a solar cell. The series resistance is lower and the power conversion efficiency is higher for InGaN devices grown with an AlN buffer layer.

1 Introduction The band gap tuning range of the $In_xGa_{1-x}N$ ternary alloy extends from the near-infrared (x = 1.0, 0.65 eV) to the ultraviolet (x = 0, 3.4 eV) [1]. The positions of the conduction and valence band edges with respect to the vacuum level span a correspondingly wide range, as illustrated in Fig. 1. In the figure, we use a value of 1.0 eV for the valence band offset between GaN and InN [2], which corresponds to an InN electron affinity of 5.8 eV, but note a recent report of a somewhat smaller electron affinity of 5.5 eV [3]. For all values of x, the conduction band of $In_xGa_{1-x}N$ is below that of Si, and for x greater than about 0.45, it is below the valence band of Si.
There are a number of interesting InGaN/Si heterostructures that can be proposed. As shown in Fig. 2(a), an unpinned n-$In_{0.45}Ga_{0.55}N$/p-Si anisotype junction should have little band bending at the interface and efficient electron-hole recombination and ohmic behavior is predicted. This can be used as a component of an InGaN/Si tandem solar cell with the heterojunction serving as a low-resistance contact for series connection of the pn subcells [4]. Also illustrated is an ideal n-$In_{0.35}Ga_{0.65}N$/n-Si isotype junction. In this case, due to the large electron affinity of the InGaN, there is depletion on the Si side of the junction and rectifying behaviour would be predicted [5].

The performance of such heterojunction devices will depend on the quality of the InGaN layer(s) and on the properties of any interface or buffer layers. Growth of $In_xGa_{1-x}N$-based opto-electronic device structures on Si has been extensively investigated previously with the goal

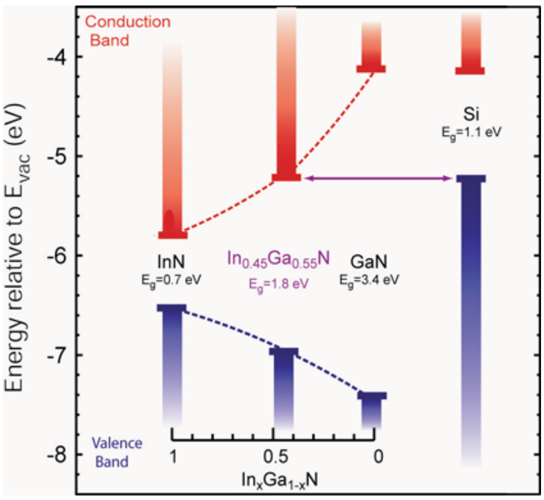

Figure 1 Absolute (relative to vacuum) valence and conduction band edge positions of $In_xGa_{1-x}N$.

of optimizing the interface layer(s) between the Si and the active layers to reduce defects in the nitride layers and to improve device performance [6]. Light emitting diode structures have been fabricated either using standard top and mesa electrical contacts to the nitride layers [7] or using n-Si as the back contact [8-10]. In this latter case, electrical transport between the Si substrate and the epilayer is crucial. Transport between Si and n-GaN thin films [11] and nanocolumns [12] has been studied before, but we are not aware of similar transport studies for monolithic InGaN structures on Si.

AlN is frequently used as a buffer layer for molecular beam epitaxy deposition of III-nitride thin films on Si [6, 7, 13-16]. It might be expected that this might have a deleterious effect on transport as AlN would be expected to be an insulator. Si_3N_4 has also been used as a buffer layer; we will report elsewhere the observation that crystalline quality is improved and the In incorporation is increased when the $In_xGa_{1-x}N$ thin films are grown with an intentional Si_xN_y buffer [17]. Here, we compare the electrical transport properties of InGaN/Si heterostructures grown on Si(111) with either an AlN or Si_3N_4 interface layer.

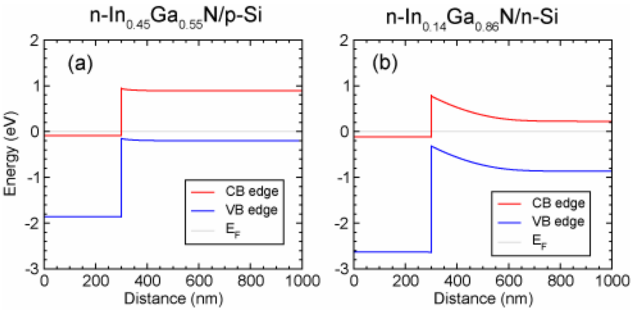

Figure 2 Calculated band alignments for $In_xGa_{1-x}N/Si$ junctions for the np (a) and nn (b) configurations. In (a), x = 0.45 and the electron concentration in the InGaN layer is $5x10^{18}$ cm^{-3}. In (b), x = 0.14 and the electron concentration in the InGaN layer is $1x10^{19}$ cm^{-3}. The carrier concentration in the Si (electrons or holes) was set at $3x10^{15}$ cm^{-3}. The assumed values of x and electron concentrations correspond to the data presented in Figs. 3 and 4(b).

2 Experimental Substrates used were either n- or p-type Si(111) or Si(100). Films with an AlN buffer layer were grown by gas source molecular beam epitaxy (GS-MBE) using an rf plasma source to generate N atoms. An AlN buffer layer from 20-130 nm in thickness was used as a buffer layer followed by growth of InGaN of the desired composition. A home-built plasma-assisted MBE system was used to grow single phase $In_xGa_{1-x}N$ (x = 0.2-0.3) using a Si_3N_4 buffer layer, which was produced by 10 min. of nitridation at 800 °C.

Film composition and stoichiometry were evaluated by X-ray diffraction and Rutherford backscattering spectrometry. For electrical characterization, sputtered indium tin oxide (ITO) was used as a top contact and Ga was used as a Si back contact for n-Si and Al was used for p-Si. The presence of the Si substrate interferes with direct electrical characterization of the InGaN layers using the Hall effect. Electron concentrations in the InGaN layers were estimated from films grown on sapphire or sapphire/GaN templates with similar values of x and are mid 10^{18} cm^{-3} for the AlN buffer layer and mid 10^{19} cm^{-3} for the Si_3N_4 buffer. Illuminated current-voltage data was obtained with a 1x AM 1.5 solar simulator. For rectifying junctions, dark and illuminated IV data were modelled using Eq. (1):

$$I = I_{sat}\left\{\exp\left[\frac{q(V-IR_s)}{nkT}\right]-1\right\}-I_L-\left[\frac{V-IR_s}{R_{sh}}\right] \qquad (1)$$

where I_{sat} is the diode saturation current, q is the charge on the electron, n is the ideality factor (assumed to be 1 here), k is the Boltzmann constant, T is the temperature (300 K for the data here), I_L is the current due to the illumination, R_s is the series resistance, and R_{sh} is the shunt resistance [18]. Reported values for area specific series and shunt resistances were obtained by multiplying R_s and R_{sh} by the contact area.

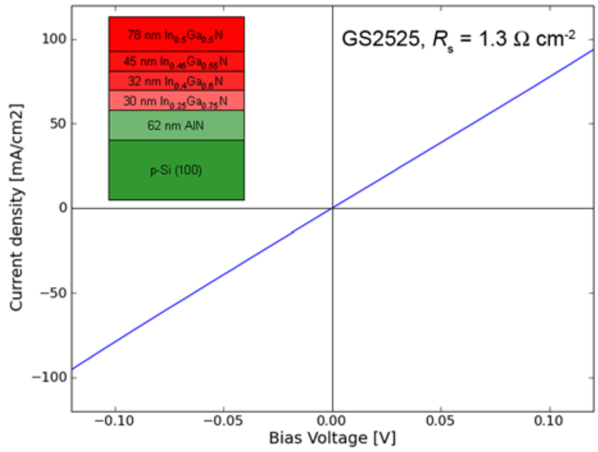

Figure 3 IV measurements of a n-$In_xGa_{1-x}N$/p-Si(100) heterostructure with a 62 nm AlN interface. Although there is a thin layer of Ga-rich material near the junction, most of the structure has x ~ 0.45, corresponding to the band alignment shown in Fig. 2(a).

3 Results and discussion Figure 3 shows the structure and IV characteristics of an n-$In_xGa_{1-x}N$/p-Si(100) heterostructure. As illustrated in the inset, the RBS analysis reveals a 62 nm thick AlN layer. Although most of the layer has x ~ 0.45, there is an In-depleted layer on top of the AlN. The junction is ohmic, as predicted, with a low specific series resistance of 1.3 Ωcm^2. Similarly low series resistances have been obtained for AlN buffer layers as thick as 130 nm. We observed the predicted ohmic behaviour for n-$In_xGa_{1-x}N$/p-Si(111) structures grown with a Si_3N_4 interface layer for 0.15 < x < 0.25 but found that the series resistance is considerably higher [17].

Figure 4 compares current voltage data (dark and illuminated with AM 1.5) for n-InGaN/n-Si structures with AlN and Si_3N_4 interface layers. For the AlN interlayer, the junction is rectifying, and it has an illuminated open circuit voltage of 0.45 V and an efficiency at an short circuit current of 14.8 mA cm^{-2} of 4.5%. Temperature-dependent IV and electron induced current (EBIC) measurements [5] indicate that the voltage may be due to a pn junction formed by Al in-diffusion into the Si, similar to what has been reported earlier for AlN [19] and GaN [11] grown on Si (both Al and Ga are acceptors in Si). The n-$In_{0.4}Ga_{0.6}N/Si_3N_4$/n-Si structure has a 10 nm or thinner Si_3N_4 buffer layer, as determined by RBS. It is also rectifying, but with a smaller short circuit current and open circuit voltage. The fits to Eq. (1) are also shown for both cases. The series resistance is >10x larger for the Si_3N_4 buffer (40 vs. 3 Ω cm^{-2}) and there is evidence of photoconductivity under illumination. Also, there is slope change under forward bias which may reflect a change in the ideality factor or the presence of other barriers in the device [20].

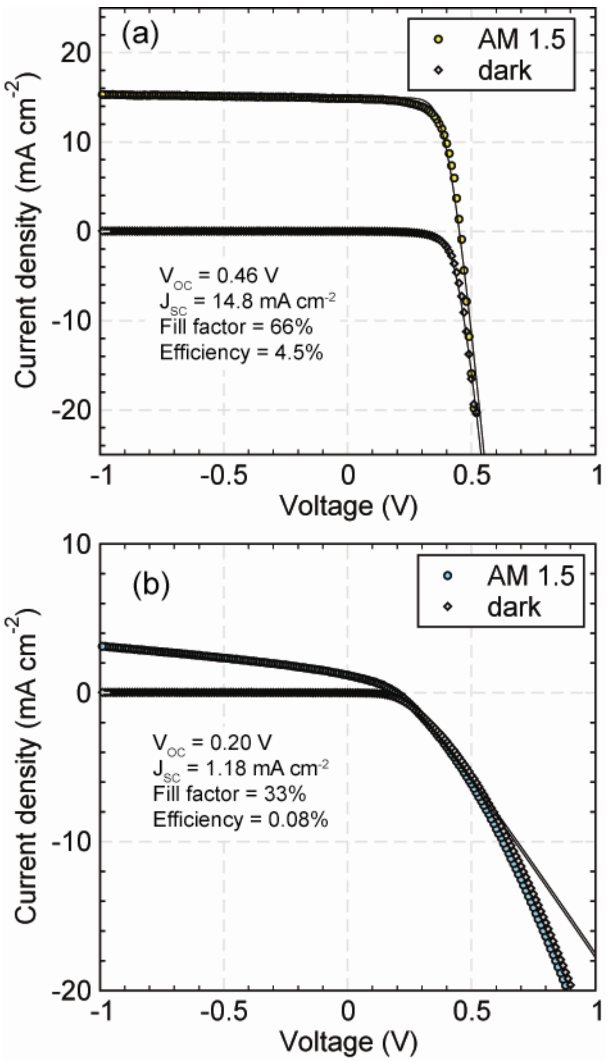

Figure 4 Dark and illuminated current-voltage measurements of n-$In_xGa_{1-x}N$/n-Si heterostructures. (a) 110 nm $In_{0.27}Ga_{0.62}N$ layer/ 40 nm AlN/n-Si(111), GS2435. (b) 400 nm $In_{0.14}Ga_{0.86}N$/10 nm Si_3N_4/n-Si(111), IGN43. The solid lines are the fits to Eq. (1).

Temperature-dependent IV measurements were performed on the sample with the Si_3N_4 buffer layer over the T range 300–370 K. In this case, we do not believe there is doping of the Si, as with the AlN buffer, so the barrier is due to the depletion of the n-Si by the InGaN. Analysis of the forward current as a function of temperature was performed using the standard Schottky diode analysis [18]. The estimated barrier height is 0.6 eV, which is consistent with the band diagram shown in Fig. 2(b).

The larger resistances of the devices with the 40 nm Si_3N_4 layer are not surprising, as we expect this layer to be insulating. Also, we do not expect that there is dopant in-diffusion. However, the low forward resistance of the AlN interface device is surprising, given that AlN with its >6 eV bandgap, would be expected to be insulating. This effect has been observed before in GaN LED structures grown on Si with a thinner (8-10 nm) AlN buffer layer and was attributed to electron conduction along threading dislocations [8, 9]. Here, we suspect that doping of the AlN by Si [21] or conduction via native defects may also play a role.

4 Conclusions For MBE-grown $In_xGa_{1-x}N$ films with x in the range of 20-30%, ohmic junctions are formed with p-type Si and rectifying junctions are formed with n-type Si. Thick AlN layers (up to 85 nm) do not appear to be a significant source of series resistance, in spite of the expected insulating behaviour. The series resistance of devices made with a thin Si_3N_4 buffer is about 10x higher.

Acknowledgements Work at LBNL was supported by Rose Street Energy Laboratory (JWA, LAR, KMY) and by the Office of Science, U.S. Department of Energy under Contract No. DE-AC02-05CH11231 (YR, DK, SRL). Y. Cui acknowledges fellowship support from the Sea Change Foundation.

References

[1] W. Walukiewicz, J. W. Ager III, K. M. Yu, Z. Liliental-Weber, J Wu, S. X. Li, R. E. Jones, and J. D. Denlinger, J. Phys. D **39**, R83 (2006) and refs. therein.
[2] G. Martin, A. Botchkarev, A. Rockett, and H. Morkoç, Appl. Phys. Lett. **68**, 2541 (1996).
[3] C.-L. Wu, H.-M. Lee, C.-T. Kuo, S. Gwo, and C.-H. Hsu, Appl. Phys. Lett. **91**, 042112 (2007).
[4] J. W. Ager III, L. Reichertz, D. Yamaguchi, L. Hsu, R. E. Jones, K. M. Yu, N. Miller, W. Walukiewicz, and W. J. Schaff, in: Proceedings of the 22nd European Photovoltaic Solar Energy Conference, Milan, Italy, 2007 (WIP-Renewable Energies, Munich, 2007), pp. 215–218.
[5] J. W. Ager III, L. A. Reichertz, K. M. Yu, W. J. Schaff, T. L. Williamson, M. A. Hoffbauer, N. M. Haegel, and W. Walukiewicz, in: Proceedings of the 33rd Photovoltaic Specialists Conference, San Diego, USA (IEEE, 2008).
[6] A. Krost and A. Dadgar, Mater. Sci. Eng. B **93**, 77 (2002) and refs. therein.
[7] M. A. Sánchez-García, F. B. Naranjo, J. L. Pau, A. Jiménez, E. Calleja, E. Munõz, J. Appl. Phys. **87**, 1569 (2000).

[8] S. Guha and N. A. Bojarczuk, Appl. Phys. Lett. **72**, 415 (1998).
[9] J.W. Yang, A. Lunev, G. Simin, A. Chitnis, M. Shatalov, M. A. Kahn, J. E. Van Nostrand, and R. Gaska, Appl. Phys. Lett. **76**, 273 (2000).
[10] A. Ohtani, K.S. Stevens, and R. Beresford, Appl. Phys. Lett. **65**, 61 (1994).
[11] E. Calleja, M. A. Sánchez-García, D. Basak, F. J. Sánchez, F. Calle, P. Youinou, E. Munõz, J. J. Serrano, J. M. Blanco, C. Villar, T. Laine, J. Oila, K. Saarinen, and P. Hautojärvi, C. H. Molloy and D. J. Somerford, and I. Harrison, Phys. Rev. B **58**, 1550 (1998).
[12] A. Kikuchi, M. Kawai, M. Tada, and K. Kishino, Jpn. J. Appl. Phys. **43**, L1524 (2004).
[13] M. Godlewski, J. P. Bergmann, B. Monemar, U. Rossner, and A. Barski, Appl. Phys. Lett. **69**, 2089 (1996).
[14] P. Deelman, R. Bicknell-Tassius, S. Nikishin, V. Kuryatkov, and H. Temkin, Appl. Phys. Lett. **78**, 2172 (2001).
[15] T. Yamaguchi, Y. Saito, C. Morioka, K. Yorozu, T. Araki, A. Suzuki, and Y. Nanishi, Phys. Status Solidi B **240**, 429 (2003).
[16] C.-L. Wu, C.-H. Shen, H.-W. Lin, H.-M. Lee, and S. Gwo, Appl. Phys. Lett. **87**, 241916 (2005).
[17] Y. E. Romanyuk, D. Kreier, Y. Cui, K. M. Yu, J. W. Ager III, and S. R. Leone, under preparation.
[18] S. M. Sze, Physics of Semiconductor Devices, 2nd ed. (Wiley, New York, 1981), pp. 279–286 and 790–807.
[19] X. Zhang, D. Walker, A. Saxler, P. Kung, J. Xu, and M. Razeghi, Electron. Lett. **32**, 1622 (1996).
[20] J. M. Shah, Y.-L. Li, Th. Gessmann, and E. F. Schubert, J. Appl. Phys. **94**, 2627 (2003).
[21] M. Hermann, F. Furtmayr, A. Bergmaier, G. Dollinger, M. Stutzmann, and M. Eickhoff, Appl. Phys. Lett. **86**, 192108 (2005).